Experimental Study on the Drift-Alfvén Modes in a Collisional Current-Carrying Finite-β Plasma

Tetsuya AKITSU and Masaaki INUTAKE[1)]

University of Yamanashi, Professor EMERITUS, 4-3-11 Takeda, Kofu, Yamanashi 400-8511, Japan
[1)]*Tohoku University, Professor EMERITUS, 6-6-4 Aoba, Aoba-Ku, Sendai, Miyagi 980-8579, Japan*

(Received 22 March 2022 / Accepted 6 May 2022)

A surface-localized mode governing resistive drift-Alfvén mode is experimentally observed in a collisional, current-carrying finite-β plasma, accompanied by an electron diamagnetic-drift frequency spectrum. The half-wavelength travelling along the plasma column with the Alfvén velocity determines the Alfvén mode. The spatial distribution and the phase relation of magnetic components are presented.

Keywords: Drift-Alfvén instability, finite-β plasma

DOI: 10.1585/pfr.17.1401081

1. Introduction

L-H transition [1, 2] drew attention to instabilities in finite β plasmas, where the kinetic pressure of plasma is a significant fraction of the confining magnetic field energy density. Edge-localized mode (ELM) is an effect observed around the plasma in an improved confinement mode known as H mode, and is increasingly attracting attention [3–5]. A comprehensive review of the ELM [6] and Tokamak plasma confinement and transport [7] has been reported. The roles of the low-frequency instabilities, in the deterioration of the plasma confinement have not been experimentally identified. ELM such as electrostatic drift wave or electromagnetic drift-Alfvén instability have not been studied. When the growth rates of the unstable mode are plotted as a function of the plasma current, two opposing effects can be observed. One effect is the destabilization of the drift-Alfvén coupled mode, and another effect may be the stabilization due to the poloidal magnetic field. In laboratory plasmas, Tang and Luhmann Jr. investigated the current driven drift-Alfvén instability, in UCLA, differentially-pumped arc-jet, and Nishida and Ishii investigated the same mode in a test plasma with direct-current (TPD), thermionic emission plasma source in [8–10]. We aimed to demonstrate the drift-Alfvén coupled modes observed in a test plasma with a high density (TPH) device at the Institute of Plasma Physics. Afterwards, the spectral analysis in the arc-jet experiment was established in the study on the propagation characteristics of non-axisymmetric Alfvén wave by Amagishi *et al.* [11], and current-driven Alfvén instability by Hatakeyama *et al.* [12] in a flat-top 4 ms, quasi-steady state of the pulsed arc-jet plasma.

Miyato *et al.* demonstrated a coupled model of resistive drift-Alfvén waves destabilized in a current-free magnetized plasma and the eigenfunction for the electric potential and magnetic vector fluctuations localized in the edge plasma in [13, 14] and the plasma current effects on the unstable resistive drift-Alfvén modes [15, 16]. Miyato *et al.* introduces an electric and magnetic vector eigenmode in a current driven drift-Alfvén mode and the behavior in a poloidal magnetic field, with a large axial current. The eigenfrequency continuously changes as the axial current increases

In this study, we introduced the spatial distribution of the fundamental mode of the drift branch and higher mode of the current-driven drift-Alfvén mode in a smaller axial current.

2. Experimental Apparatus and Results

Figure 1 shows the experimental arrangement of the current drive of the low frequency electromagnetic instability, in the TPH device. A magneto-plasma dynamic arc-jet excited quasi-steady, current-less plasma in a uniform magnetic field $B_0 \leq 0.32$ T. Typical experimental parame-

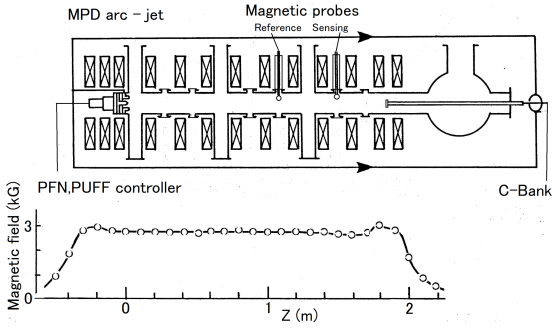

Fig. 1 A schematic of the TPH experiment. MPD stands for the magneto-plasma-dynamic arc jet which injects high density helium plasma. C-Bank: Auxiliary capacitor bank.

author's e-mail: akitsutetsuyadr.eng@gmail.com

Table 1 Characteristic parameters of the TPH plasma.

Magnetic field	$B_0(\mathrm{T}) = 0.3$
Radius	$a(\mathrm{m}) = 0.05$
Plasma column length	$L(\mathrm{m}) = 2$ m
Ion cyclotron frequency	$f_{ci} = 1.15$ MHz
Electron and ion temperatures	$T_i \sim T_e \sim 4$ eV
Plasma density	$n_e \sim 4 \times 10^{14}$ cm^{-3}
Resistivity	$\eta_\parallel \sim 5 \times 10^{-5}$ Ωm, $\eta_\perp \sim 2\eta_\parallel$
Plasma flow speed	$U \sim 10^6$ cm/s
Alfvén speed	$V_A \sim 1.5 \times 10^7$ cm/s
Ion acoustic speed	$C_s \sim 10^6$ cm/s
Electron thermal speed	$V_{Te} \sim 10^8$ cm/s
Ionization degree	$\gtrsim 70$ %, (−fully ionized)
Estimated β-value	0.8 %

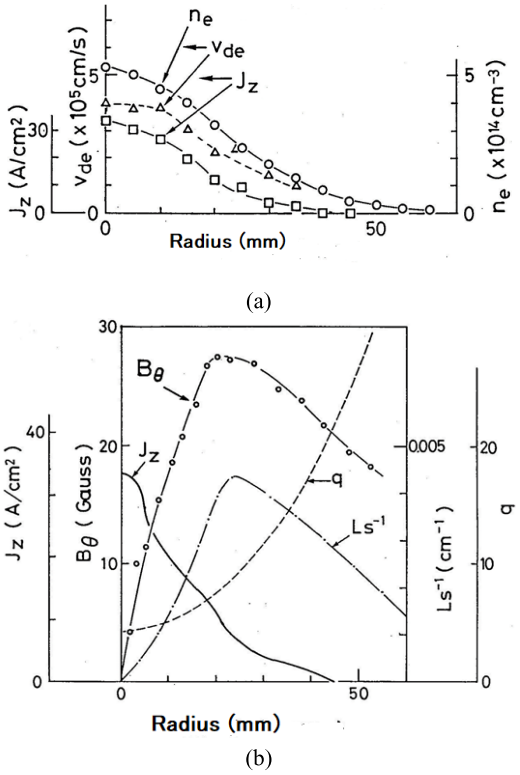

Fig. 2 A typical profile of the plasma, (a) the radial distribution of the plasma density, current density and v_{de}, (b) the radial distribution of the current and the induced magnetic field. L_s^{-1}, $q = 2\pi r B_{0z}/LB_{0\theta} \geq 5$.

ters are summarized in Table 1. The drift-Alfvén instability was excited by a target electrode that was positively polarized using an auxiliary capacitor bank. A pulse forming network provided discharge current and a PUFF controller controlled the gas flow. The recombined gas is exhausted through three lateral ducts extending laterally and a cylindrical container near the end. During the flat-top 4 ms, an axial current pulse was aligned and the magnetic field perturbation was detected using two magnetic probes ar-

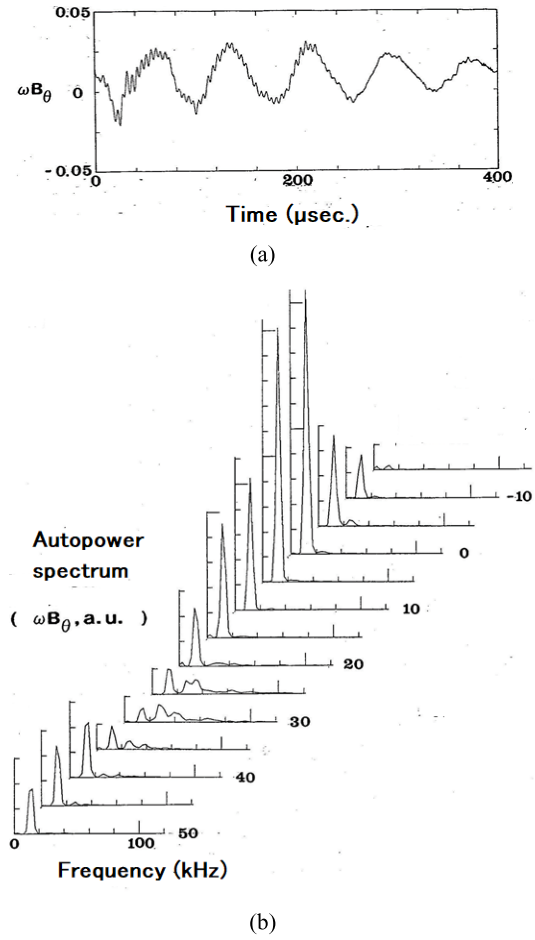

Fig. 3 A typical profile of the distribution of the perturbed magnetic field, (a) $\omega\tilde{B}_\theta$ at the plasma center, (b) distribution along the horizontal axis. $I_T = 0.4396$ kA.

ranged along the equilibrium magnetic field. The signal was digitized and converted into the frequency domain using high-speed Fourier conversion. The Hamming window function is used to correct the finite-length time window effect. The phase difference in the complex component provides information on propagation speed and, notably the propagation direction.

Figure 2 shows a typical plasma density, axial electron drift, and induced magnetic field distribution in the radial direction. The auxiliary capacitor bank voltage controls the axial current as $I_T = 0.1 + 0.167V_T$, where I_T is the axial current, V_T the charging voltage.

Figure 3 shows a frequency spectrum of $\tilde{B}_\theta$ at different horizontal positions. The primary result of this study is the observation of the high-frequency component at $r = 25$, 30 mm, and the spatial distribution is shown in Figs. 4 and 5.

Similarly, the diamagnetic signal $\tilde{B}_z$ was measured and the pressure of the magnetic field expelled by the plasma was 269 N/m^2. The magnetic pressure of the equilibrium magnetic field was 3.57×10^4 N/m^2, which corresponded to the β value 8×10^{-3}.

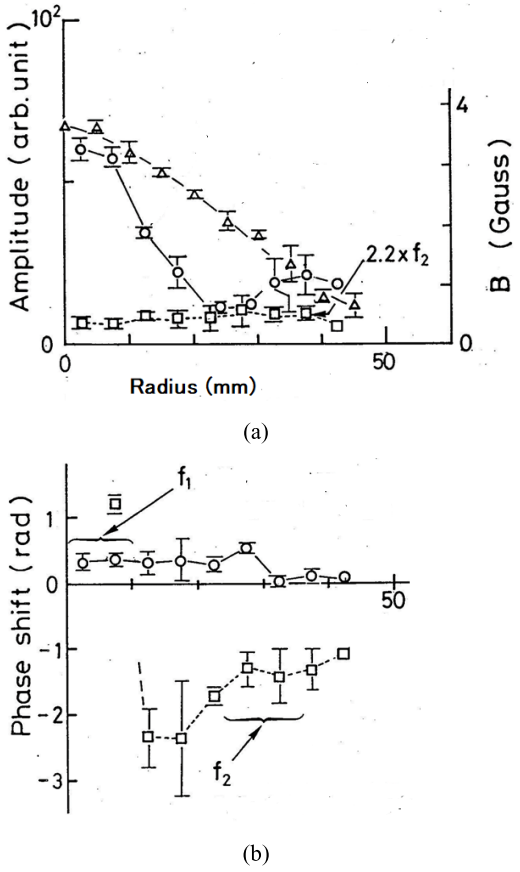

Fig. 4 Spatial distribution of the perpendicular component. (a) Amplitude. Circles: B_θ; Triangles: $B_r, f_1 = 12.2$ kHz; Square symbols: B_θ, 26.9 kHz; (b) Phase shift. Circles: B_θ $f_1 = 12.2$ kHz, $0.74 - 1.35 \times 10^7$ cm/s, upstream, against the axial electron drift; Square symbols: B_θ, 26.9 kHz, $3.9 - 6.8 \times 10^7$ cm/s, downstream, along the axial electron drift.

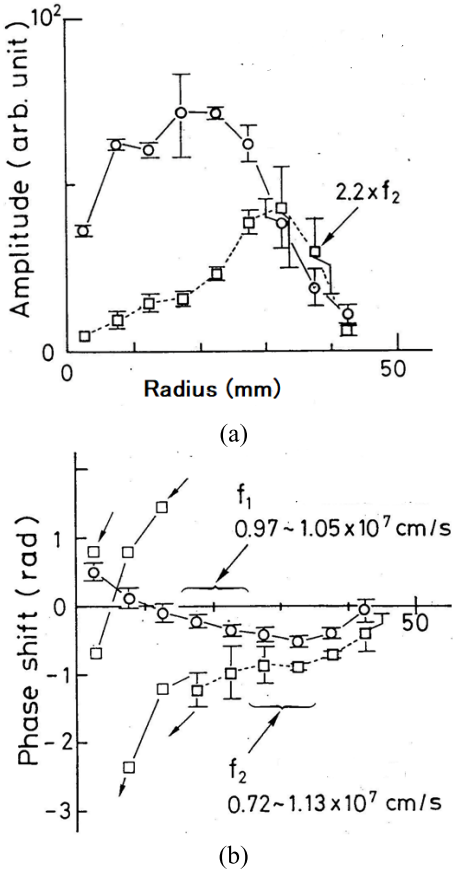

Fig. 5 Spatial distribution of B_z component. (a) Amplitude. Circles: B_z; $f_1 = 12.2$ kHz; Square symbols: B_z, 26.9 kHz; (b) Phase shift. Circles: B_z $f_1 = 12.2$ kHz, $0.97 - 1.05 \times 10^7$ cm/s, downstream, parallel to the axial electron drift; Square symbols: B_z, 26.9 kHz, $0.72 - 1.13 \times 10^7$ cm/s, downstream, parallel to the axial electron drift.

The half wavelength of the Alfvén mode corresponds to the plasma length in the eigenmode for $m = 1$, $n = 1$ resonance. The resonance was not observed for the TPH device. The electron diamagnetic frequency is low, and the destabilization of the higher resonance mode is destabilized by a higher current. In Table 2, $j = 1$ and $j = 3$ are the identification numbers of eigenfunctions [15,16]. The electron diamagnetic drift is the energy source of the unstable oscillation; however, in the current-aligned case, it does not guarantee the localization of the eigenfunction. This effect modifies the growth rate of the eigenfunctions (Table 2). The effect on the modification of the eigenfunction is localized in the peripheral region of the plasma column [15]. The resonance condition is $\omega^* = \omega_A$, where $\omega_A = k_z v_A$ is the Alfvén frequency.

The resonance of the drift wave with the travelling wave of the Alfvén mode occurred, because the electron diamagnetic frequency ($m = 1$) is too low for the coupling with the half-wavelength standing wave.

ω_r/ω^*, ω_i/ω^* are the real and imaginary parts normalized by ω^*, where $\omega^* = k_y V_{Te} \rho_e / L_n$ is an electron diamagnetic frequency in a simple magnetized slab plasma model, where L_n is the scale length of the density.

Table 2 Comparison of ω_i/ω^*, ω_r/ω^*.

	Current – free	Current – aligned plasma*
$j = 1$		
ω_i/ω^*	0.084	0.104
ω_r/ω^*	0.97	0.96
$j = 3$		
ω_i/ω^*	0.21	0.23
ω_r/ω^*	0.82	0.78

*Axial current: $I_0 = 439.6$

The lower frequency component at $f_1 = 9.7$ - 12.2 kHz is detected at $r = 0$ - 25 mm. The return contour of the perturbed magnetic field is detected at $r = 35$ - 50 mm, which is the edge region surrounding the plasma column. Higher frequency component at $f_2 = 26.9$ - 40 kHz is de-

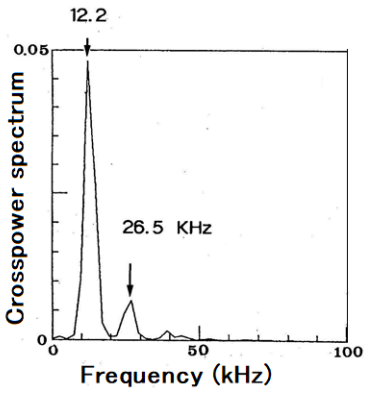

Fig. 6 Cross-power spectrum between the ion saturation current of an electrostatic probe and the magnetic perturbation, located at the edge region (r = 20 mm).

tected at r = 25 - 35 mm. The observation of the localized higher frequency component, possibly, the observed peak at f_2 is the coupled-mode Alfvén branch of the higher harmonics, within the acceptable errors. The magnitude $B_\theta \simeq B_r \simeq 4$ Gauss and $B_\theta, B_r > B_z$ are noted as in the established relations in the preceding experiments, at the electron diamagnetic frequency [8–10]. The phase shift indicates the signal flow between two magnetic probes spaced at 0.4 m intervals, along the equilibrium magnetic field line. This result shows the signal transmission in the Alfvén speed within the standard error of the ensemble average. The magnetic field fluctuation B_θ propagates in the same direction as the electron drift at f_1 and in the opposite direction at f_2. The direction of the signal flow of B_z may require further discussions.

Finally, Fig. 6 shows a cross power spectrum, which is a Fourier transform of the correlation between the fluctuation of the ion saturation current and the magnetic fluctuation. The reference magnetic probe is located at r = 20 mm, and the ion saturation current was measured with a negatively polarized double probe, at −20 V, in the edge region of the plasma column (r = 30 mm). This result indicates that the density fluctuation and the magnetic field perturbation have a high correlation at 12.2 kHz, corresponding to the fundamental mode of the drift branch (m = 1), and at 26.5 kHz.

The higher frequency peak may correspond to the coupled drift-Alfvén instability at a higher poloidal mode, (m = 3). The resonance between the Alfvén mode resonance appears in the plasma column at a larger axial current $I_T > 1.5$ kA [15].

3. Concluding Remark

In the TPH experiment conducted in the 1980s, only little was known about the low-frequency edge-localized instabilities until recently. Research on the L-H phenomena will continue to be abundant, and the low-frequency modes such as the drift waves coupled with Alfvén waves remain important when the resonance condition $\omega^* = \omega_A$, $\omega^* = k_y V_{Te}\rho_e/L_n$, $\omega_A = k_z v_A$ is satisfied.

This experiment was conducted to bridge the gap between the fundamental study of the electrostatic current-driven drift wave instability and the Tokamak experiment for confinement and transport. The spatial distribution of the magnetic fluctuation observed in the TPH experiment differs from previous studies, because of the large diameter, high-density plasma and the minimum requirement for the destabilization of the resistive drift-Alfvén instability at the target current $I_T \geq 0.3$ kA. The higher frequency magnetic fluctuation was observed in the peripheral region of the plasma column, indicating the start of spectral broadening and the turbulence.

Our results suggest that once a higher axial current is established in a larger axial current, our results suggest that radial magnetic fluctuations due to the resistive drift-Alfvén modes have a broader frequency spectrum once the higher current experiment is established, even if the one or two poloidal and toroidal (longitudinal) mode spectra are expected to be narrow. The relevant mode numbers are not large for low electron temperature laboratory plasma; however, the increase of mode numbers is significant when the plasma temperature reaches the order of the present Tokamak experiment. The frequency spectrum may also depend on the plasma current and induced poloidal magnetic field. The resistive drift-Alfvén modes may affect radial plasma transport. Future investigations on this subject are expected.

Acknowledgments

The author expresses special thanks to Dr. Naoaki Miyato, Professor Dr. Satoshi Hamaguchi, and Professor Dr. Masahiro Wakatani for fruitful discussions, to Dr. Rikizo Hatakeyama, Professor Dr. Noriyoshi Sato, Professor Dr. Ryohei Itatani, and Professor Dr. Hideo Ikegami for instructive comments, and to Mr. Shigeru. Kishimoto for his technical assistance. TPD and TPH were settlements in the Institute of Plasma Physics, Nagoya University. This work was carried out under the Collaborating Research Program. The author appreciates the research opportunity using this device under the Collaborating Research Program.

[1] B. Scott, Plasma Phys. Control. Fusion **40**, 823 (1998).
[2] R.N. Roger and J.F. Drake, Phys. Rev. Lett. **79**, 229 (1997).
[3] A.B. Mikhailovskii and L.I. Rudakov, Zh. Eksp. Teor. Fiz. 44, (912) see also A.B. Mikhailovskii, *Review of Plasma Physics*, edited by M.A. Leontovich, (Consultants Bureau, New York, 1967) Vol.III.
[4] B.B. Kadmotsev, *Plasma Turbulence* (Academic Press, London, 1965).
[5] B.B. Kadmotsev, Zh. Tech. Fiz. **31**, 1208 (1961).
[6] Y. Kamada, N. Oyama and M. Sugihara, "Various types of ELMs", J. Plasma Fusion Res. **82**, 9, 566 (2006) (in

Japanese).
[7] E.J. Doyle *et al.*, "Chapter 2: Plasma confinement and transport", Nucl. Fusion **47**, S18 (2007), doi.org/10.1088/0029-5515/47/6/S02
[8] J.T. Tang, N.C. Luhmann Jr., Y. Nishida and K. Ishii, Phys. Rev. Lett. **34**, 2, 70 (1974), doi.org/10.1103/Phys RevLett.34.70
[9] Y. Nishida and K. Ishii, Phys. Rev. Lett. **33**, 6, 352 (1974).
[10] J.T. Tang and N.C. Luhmann Jr., Phys. Fluids **19**, 1935 (1976), doi.org/10.1063/1.861410
[11] Y. Amagishi, M. Inutake, T. Akitsu and A. Tsushima, Jpn. J. Appl. Phys. **20**, 11, 2171 (1981).
[12] R. Hatakeyama, M. Inutake and T. Akitsu, Phys. Rev. Lett. **47**, 3, 183 (1981), doi.org/10.1103/PhysRevLett.47.183
[13] N. Miyato, S. Hamaguchi and M. Wakatani, J. Phys. Soc. Jpn. **69**, 5, 1401 (2000), doi.org/10.1143/JPSJ.69.1401
[14] N. Miyato, S. Hamaguchi and M. Wakatani, Contrib. Plasma Phys. **40**, 3-4, 362 (2000).
[15] N. Miyato, S. Hamaguchi and M. Wakatani, J. Phys. Soc. Jpn. **70**, 11, 3197 (2001).
[16] N. Miyato, Private communication.